Student's t test or the nonparametric Mann-Whitney test. Differences were considered significant at $p < 0.05$.

Results

Localization of pCAGGS-lacZ gene expression and serum levels of rat HGF after pCAGGS-HGF injection

To clarify the site of transgene expression, we delivered 10 μg of pCAGGS-lacZ or pCAGGS into the tail vein of normal mice. LacZ gene expression was assessed in various organs including the liver, heart, lungs, kidney, spleen, and colon. X-gal stained only in the liver of the pCAGGS-lacZ-injected mice (Figure 1A), but not in the liver of the pCAGGS-injected mice (data not shown). The stained cells were predominantly hepatocytes, which were identifiable by their polygonal shape and round nuclei, visible at a higher magnification. We did not find convincing examples of X-gal-stained cells in the heart, lungs, kidney, spleen, or colon of the pCAGGS-lacZ-injected mice (data not shown).

We also confirmed the expression of HGF in hepatocytes in the liver of mice 2 days after injection of 10 μg pCAGGS-HGF by immunofluorescence using anti-HGF antibody (Figure 1C). Expression of HGF was not detected in the liver of mice injected with pCAGGS (Figure 1D). In the liver of mice injected with pCAGGS-HGF, the expression levels of rat HGF mRNA were significantly increased, but these were not increased in mice injected with control pCAGGS (data not shown).

We next evaluated the time course of rat HGF expression after the injection of 10 μg of DNA, using a less than 3-s injection time and a volume of 2 ml. Mice were injected with either 10 μg of pCAGGS-HGF ($n = 5$) or 10 μg of pCAGGS ($n = 5$). After injection of pCAGGS-HGF, the peak plasma HGF level was 15 ± 5 ng/ml at 12 h; then it decreased gradually, and became undetectable at 60 h (Figure 1B). The plasma rat HGF levels in the control mice were not significantly increased (Figure 1B).

HGF and c-Met expression after pCAGGS-HGF injection in the colons of mice with DSS colitis

Administration of DSS did not change the time course of the plasma rat HGF level after either pCAGGS or pCAGGS-HGF injection. In other words, after injection of pCAGGS-HGF into mice with DSS colitis, the peak plasma HGF levels were at 15 ng/ml at 12 h, and then decreased gradually and became undetectable at 72 h. The plasma rat HGF levels were not significantly increased in the DSS colitis mice injected with the empty pCAGGS.

Next we evaluated the expression of HGF and c-Met in colon tissues of mice with DSS colitis by immunofluorescence at day 2 after gene transfer. HGF expression was not detected in the colons of mice injected with either pCAGGS or pCAGGS-HGF. In contrast, c-Met expression was detected in epithelial cells of the crypts of the colons of both groups (Figures 1E and 1F). The number of c-Met-positive epithelial cells was greater in pCAGGS-gene transferred mice, and stronger expression was detected in the epithelial cells of the apical side of the crypt.

HGF gene transfer protected mice from DSS colitis

To determine the effect of HGF gene transfer on colon injury, we injected 10 μg of pCAGGS-HGF or pCAGGS into the tail veins of mice before DSS administration. Mice injected with control vector pCAGGS showed 10–20% weight loss, together with diarrhea, and gross bleeding; however, pCAGGS-HGF injection ameliorated clinical disease severity from day 1 to day 4 (Figure 2A). The decrease in colon length reflects the extent of colon damage in the model, and it was minimal in mice with HGF gene transfer at days 2, 5, and 6 compared with the mice injected with control vector (Figure 2B).

In mice injected with pCAGGS, broad mucosal ulceration and degeneration, and inflammatory cellular infiltration were observed, and these lesions progressed with time (Figures 2C–2I). Inflammatory cells were infiltrated to the colon progressively with time in mice with DSS colitis which were injected with pCAGGS; however, pCAGGS-HGF injection significantly reduced the number of inflammatory cells in the colon of mice with DSS colitis (Figure 2J).

The crypt length was decreased in colitis mice injected with pCAGGS. In contrast, HGF gene transfer prevented the shortening of crypt in DSS colitis (Figure 2K).

The effect of HGF gene transfer on immune cell trafficking into the colon of DSS colitis

An immunofluorescence study revealed that DSS-induced mucosal inflammation was accompanied by a significant infiltration of Mac-1+ macrophages, CD4+ T cells, CD8+ T cells, and B220+ cells in the lamina propria of mice injected with the empty pCAGGS (Figures 3A–3D, 3I). The numbers of these immune cells were significantly reduced in mice after HGF gene therapy (Figures 3E–H, 3I).

The effect of HGF gene transfer on cytokine mRNA expression in the colons of mice with DSS colitis

To reveal the immune response in the colon of mice with DSS colitis, we analyzed the expression of mRNA of several cytokines. At day 2 after induction of colitis, the levels of expression of the mRNAs for proinflammatory

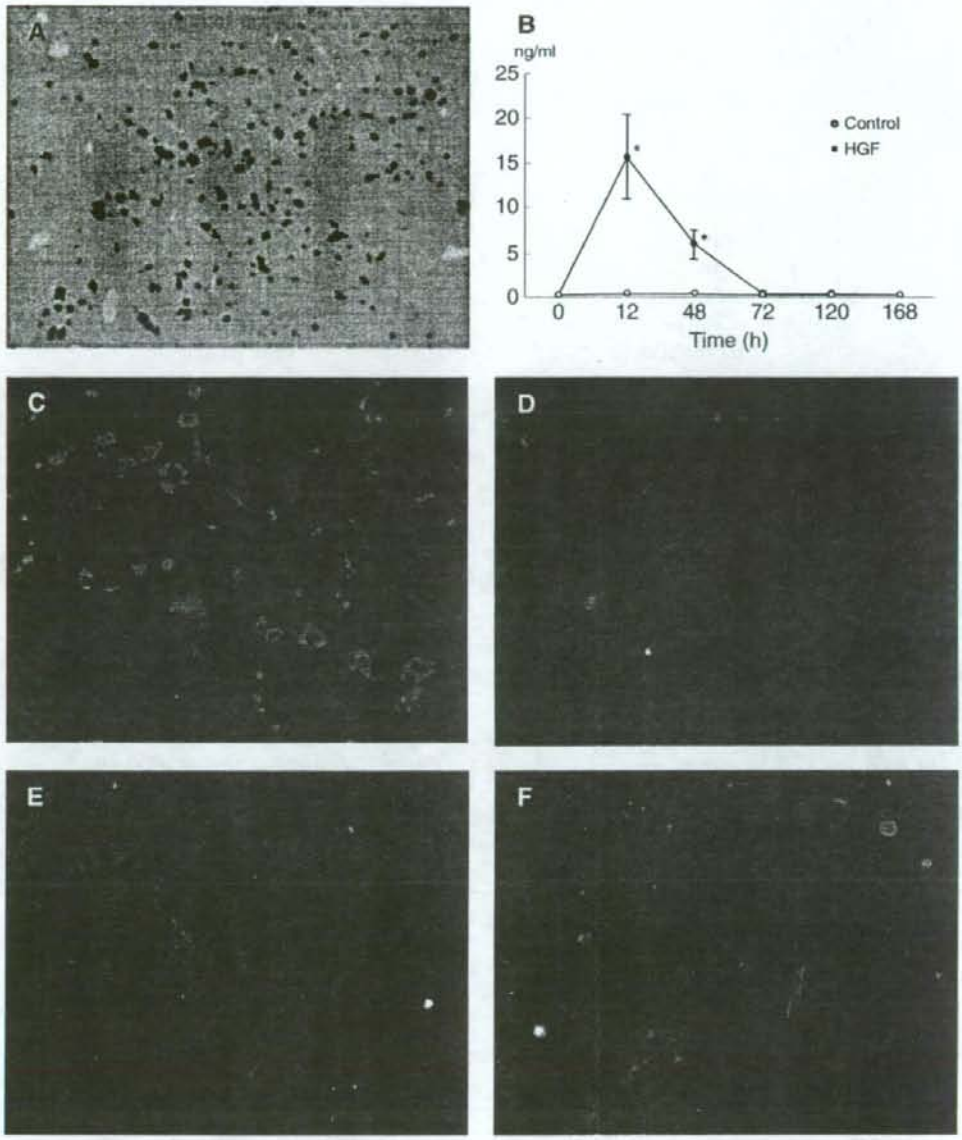

Figure 1. HGF gene transfection into the liver elevated serum HGF in mice. (A) X-gal-stained mouse liver section 1 day after injection with pCAGGS-lacZ. Original magnification: ×30. (B) Plasma levels of HGF at various time points. Blood samples were collected at 12, 48, 72, 120, and 168 h after pCAGGS-HGF injection following administration of DSS, and were detected by polyclonal HGF ELISA. Data are expressed as mean (SD), n = 10. *$p < 0.01$ versus control. (C) HGF expression was detected by immunofluorescence in the livers of mice with DSS colitis, which were injected with pCAGGS-HGF. (D) HGF was not detected by immunofluorescence in control, pCAGGS-injected mice. (E, F) c-Met, the receptor for HGF, was detected on colonic epithelial cells of mice with DSS colitis by immunofluorescence, and its expression was elevated slightly in mice injected with pCAGGS-HGF (E) compared with pCAGGS-injected mice (F)

cytokines such as IL1-β, IL18, and IFN-γ were increased, and those of TNF-α were increased at day 6 (Figure 3J). HGF gene transfer clearly reduced the expression of mRNAs for these cytokines (Figure 3K). Expression of IL-4 mRNA was increased slightly, but there was no statistical difference between mice injected with pCAGGS and those with pCAGGS-HGF (Figure 3K). Interestingly, expression of mRNA of IL-10, which is known to be an anti-inflammatory cytokine, was increased markedly at day 6 in the colons of both groups of mice; however,

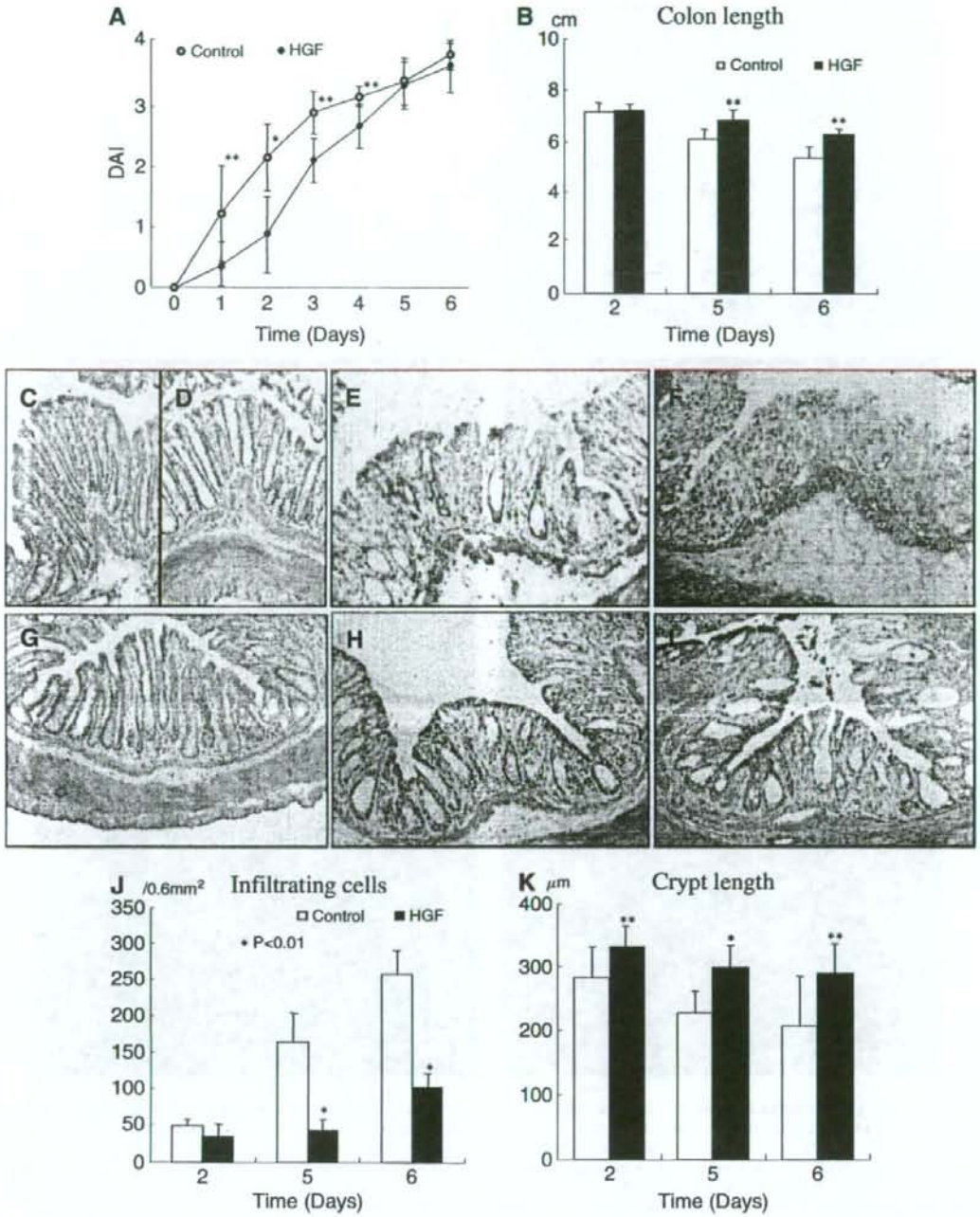

Figure 2. HGF gene transfer protected mice from acute colitis induced by DSS. (A) Disease activity index (DAI). Open circles, control pCAGGS-injected mice; closed circles, pCAGGS-HGF-injected mice. (B) Colon length, at days 2, 5, and 6. Open bars, control-pCAGGS; closed bars, pCAGGS-HGF. (C–I) Distal colon tissues: (C) from a normal mouse; (D) from pCAGGS-injected mice on day 2, (E) day 5, (F) and day 6 after DSS; and from pCAGGS-HGF-injected mice on day 2 (G), day 5 (H), and (I) day 6 after DSS. (J–K) Histological scores of colitic lesions. (J) The number of infiltrating cells in the lamina propria of the colon, at days 2, 5, and 6 after DSS. Open bars, from pCAGGS-injected mice; closed bars, pCAGGS-HGF-injected mice. (K) The crypt length of colon of mice, at days 2, 5, and 6 after DSS. Open bars, from pCAGGS-injected mice; closed bars, pCAGGS-HGF-injected mice. $^{*}p < 0.01$; $^{**}p < 0.05$

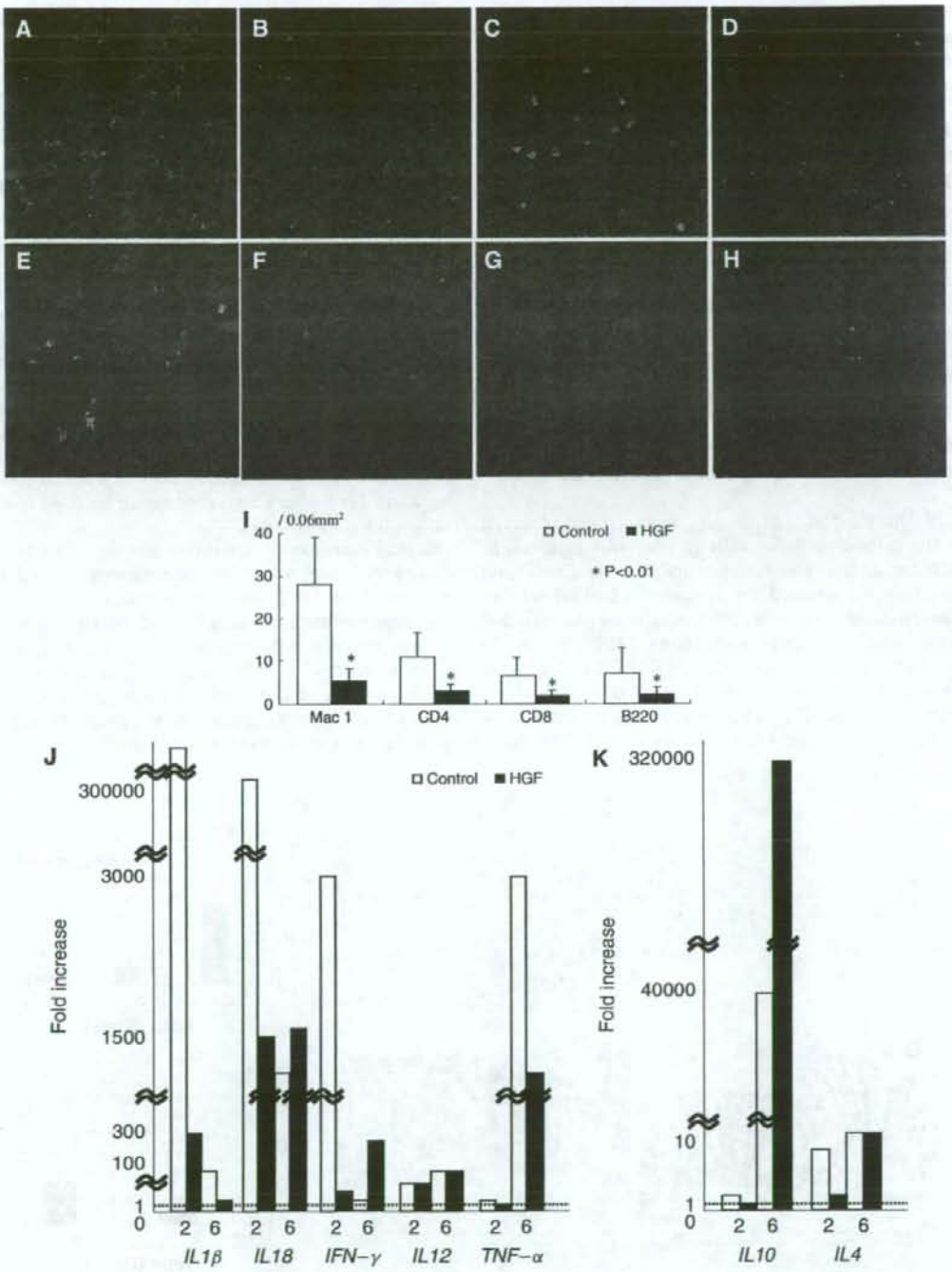

Figure 3. HGF transfection into the liver blocked immune cell traffic into the colon. (A–H) Immunostaining for Mac-1 (A, E), CD4 (B, F), CD8 (C, G), and B220 (D, H) of the distal colon tissues from pCAGGS-injected mice (A–D), and pCAGGS-HGF-injected mice (E–H). (I) Quantitative analysis of immune cells that infiltrated the colon. *$p < 0.01$. (J, K) Real-time quantitative PCR of pro-inflammatory and anti-inflammatory cytokines mRNA expression in the colon tissue. Open bars, from pCAGGS-injected mice; closed bars, pCAGGS-HGF-injected mice. Each amount was normalized to the level of GAPDH and the final relative values were expressed relative to the calibrators on day 0

HGF gene therapy significantly increased the expression level of IL-10 mRNA compared with the control vector (Figure 3K).

HGF gene transfer enhanced the proliferation of crypt epithelial cells in DSS colitis

We assessed the BrdU incorporation to evaluate the mitogenic effect of HGF on colonic epithelial cells in the amelioration of DSS colitis. BrdU+ cells were detected at the basal side of a crypt in the colon of mice with DSS colitis (Figures 4A and 4B); however, their numbers were much greater in mice that received HGF gene therapy than that of control vector (Figure 4C).

HGF gene transfer protected colonic mucosa from apoptosis in DSS colitis

As we have reported previously, apoptosis was observed in the colonic epithelial cells of mice with DSS colitis. HGF has an anti-apoptotic activity on several cells, and therefore we assessed the apoptotic epithelial cells in the colons of mice with DSS colitis using the terminal transferase uridyl nick endlabeling (TUNEL) method to detect DNA fragmentation *in situ*. TUNEL-positive colonic epithelial cells were observed along the crypts (Figures 4D and 4E), but their numbers were significantly reduced in mice that were transferred the HGF gene in comparison with that in control vector transferred mice (Figures 4D–4F).

Repeated injection of pCAGGS-HGF maintained peak levels of serum HGF longer and enabled a better cure of DSS colitis by facilitating regeneration and inhibiting apoptosis of crypt epithelial cells

Although HGF gene therapy could ameliorate acute colitis as described above, the benefit of the therapy is limited. The level of serum HGF is elevated within 3 days of a single injection of pCAGGS-HGF, and we speculated that maintenance of the elevated HGF level could induce a better therapeutic effect on colitis. We next injected pCAGGS-HGF twice, and the serum HGF level reached a peak at 12 h after the first gene injection, and decreased slightly, but was maintained at a level of 8 ng/ml during day 2 and day 5 after a second administration, 48 h after the first injection (Figure 5).

Clinical scores such as the DAI and the colon length of mice with DSS colitis were significantly ameliorated with the repeated HGF gene transfer compared to a single time administration (Figures 6A and B). Histologically, repeated injection of the HGF gene ameliorated the colitic lesions better than a single injection (Figures 6C–6F).

The numbers of BrdU-positive epithelial cells in the crypts of the colons were greater in mice injected with HGF twice than that of single injection (Figures 7A–7C). The

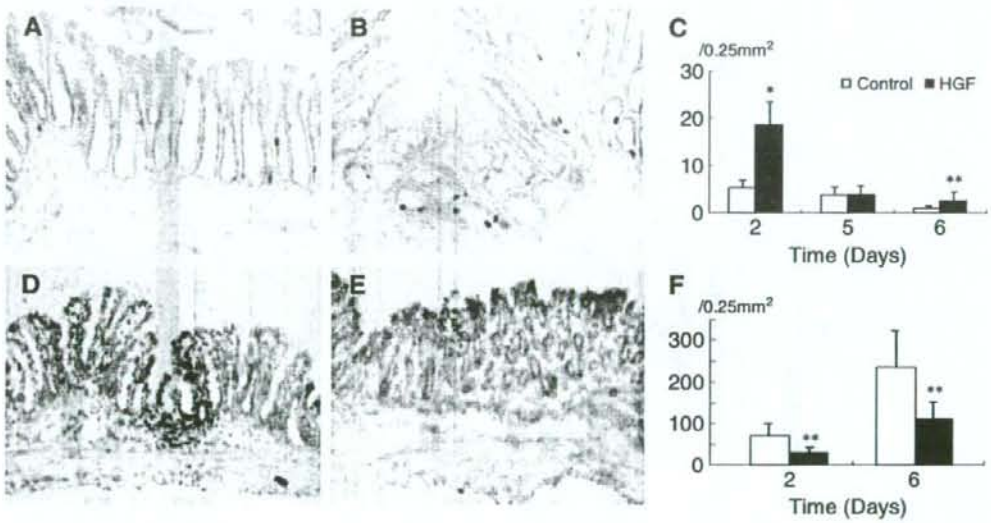

Figure 4. HGF gene transfection into the liver promoted proliferation and inhibited apoptosis of epithelial cells of the colon. (A–C) BrdU staining of distal-colon tissues from pCAGGS-injected mice (A), and pCAGGS-HGF-injected mice (B) at day 2 after DSS administration. The number of BrdU+ colonic epithelial cells (C). Open bars, from pCAGGS-injected mice; closed bars, pCAGGS-HGF-injected mice. (D–F) TUNEL staining of the distal colon tissues from pCAGGS-injected mice (D), and pCAGGS-HGF-injected mice (E) at day 2 after DSS administration. The number of TUNEL-positive apoptotic colonic epithelial cells (F). Open bars, from pCAGGS-injected mice; closed bars, pCAGGS-HGF-injected mice. *$p < 0.01$; **$p < 0.05$

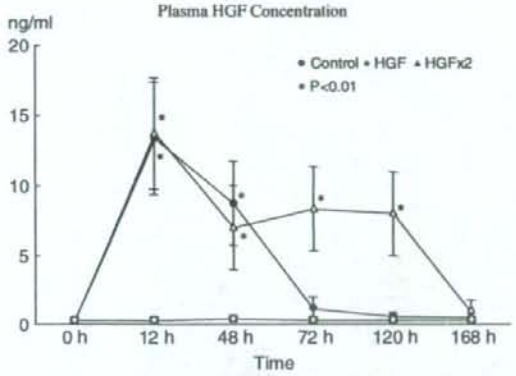

Figure 5. Repeated injection of pCAGGS-HGF kept the elevated level of plasma HGF. Plasma levels of HGF at various time points. Blood samples were collected at 12, 48, 72, 120, and 168 h after the first pCAGGS-HGF injection, and were detected by polyclonal HGF ELISA. pCAGGS-HGF was injected at 0 and 48 h after DSS administration. Open circles, pCAGGS-injected mice; closed circles, pCAGGS-HGF-injected once on day 0; open triangles, pCAGGS-HGF was injected on days 0 and 2 after DSS administration. Data are expressed as mean (SD), n = 10. *$p < 0.05$ versus control

number of TUNEL-positive apoptotic colonic epithelial cells was also reduced markedly in mice injected twice compared with mice with a single injection (Figures 7D–F).

The effect of HGF on cytokine mRNA expression in the colonic explants of mice with DSS colitis

To reveal the direct effect of HGF on immune response in the colon, we analyzed the expression of mRNA of IFN-γ and IL-10 in the colonic explants of mice with DSS colitis. In explants from mice with DSS colitis at days 2 and 5, the levels of expression of the mRNA of IFN-γ, a pro-inflammatory cytokine, was increased (Figure 8). The expression of mRNA of IFN-γ was clearly reduced by the treatment with HGF on explants (Figure 8). Expression of mRNA of IL-10, which is a known anti-inflammatory cytokine, was increased markedly at days 2 and 5 in the *ex vivo* colon tissue cultured with HGF (Figure 8). Interestingly, the expression of mRNAs for intrinsic mouse HGF and c-Met was clearly increased in explants cultured with HGF (Figure 8).

Discussion

There are various gene delivery systems, and the most intensely studied methods utilize viral vectors. There are concerns about the possibility of recombination with endogenous virus to produce a deleteriously infectious form. It has also been reported that T-cell leukemia

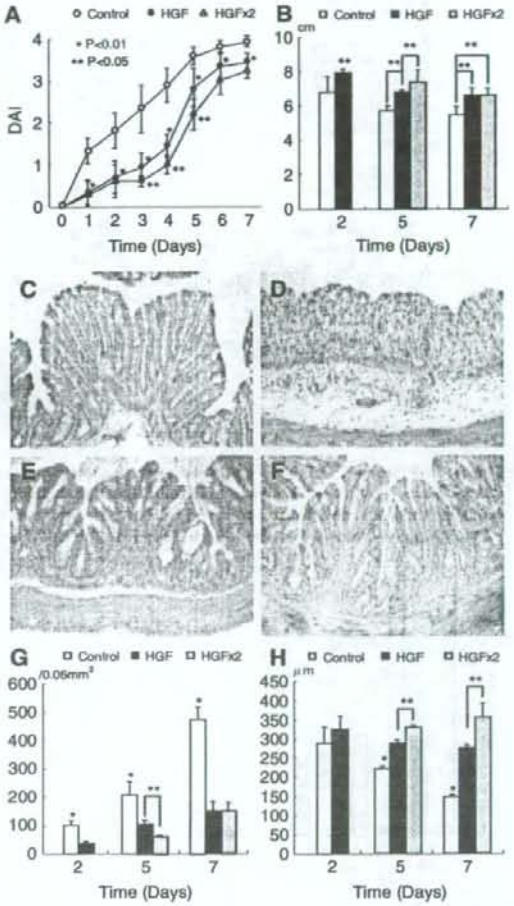

Figure 6. Repeated HGF gene transfer protected mice better from acute colitis induced by DSS. (A) Disease activity index (DAI). Open circles, control pCAGGS-injected mice; closed circles, pCAGGS-HGF-injected mice; open triangles, pCAGGS-HGF was injected on days 0 and 2 after DSS administration. (B) Colon length, at days 2, 5, and 7. Open bars, control pCAGGS; closed bars, pCAGGS-HGF; gray bars, pCAGGS-HGF was repeatedly injected on day 0 and day 2 after DSS administration. (C–F) Distal colon tissues: from a normal mouse (C); from pCAGGS-injected mice on day 2 after DSS (D); from mice with pCAGGS-HGF injection once on day 0 (E); and from mice with pCAGGS-HGF injections on days 0 and 2 (F). (G, H) Histological scores of colitic lesions. (G) The numbers of infiltrating cells in the lamina propria of the colon on day 6 after DSS. Open bars, control-pCAGGS; closed bars, pCAGGS-HGF; gray bars, pCAGGS-HGF was injected on day 0 and day 2 after DSS administration. (H) The crypt length of colons of mice on days 2, 5, and 6 after DSS. Open bars, control-pCAGGS; closed bars, pCAGGS-HGF; gray bars, pCAGGS-HGF was injected on days 0 and 2 after DSS administration. *$p < 0.01$; **$p < 0.05$

developed nearly 3 years after gene therapy for SCID using a defective retroviral vector [27,28]. Thus, there are several hurdles to overcome to enable the clinical application of gene therapy with viral vectors.

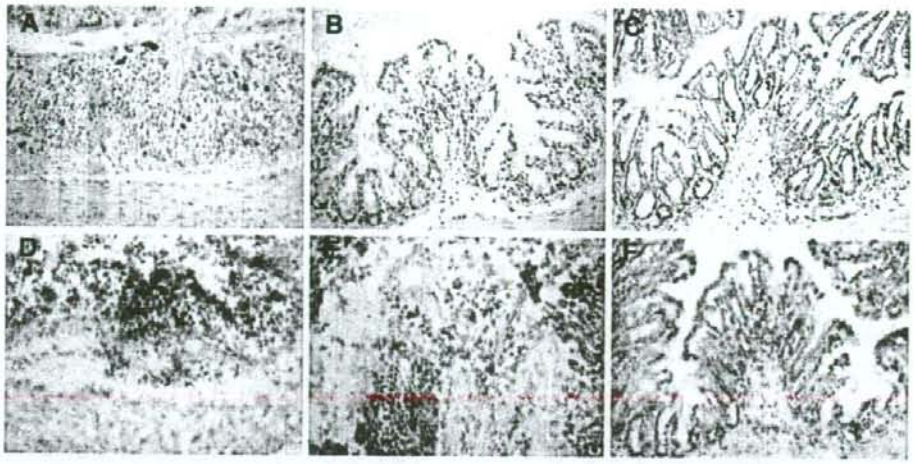

Figure 7. Repeated HGF gene transfection in the liver increasingly promoted proliferation and anti-apoptosis of epithelial cells of the colon. (A–C) BrdU staining of distal-colon tissues from a control pCAGGS-injected mouse (A), from a pCAGGS-HGF mouse injected once (B), and from a pCAGGS-HGF mouse injected twice (C). (D–F) TUNEL staining of the distal-colon tissues from a pCAGGS-injected mouse (D), from a pCAGGS-HGF mouse injected once (E), and from a pCAGGS-HGF mouse injected twice (F)

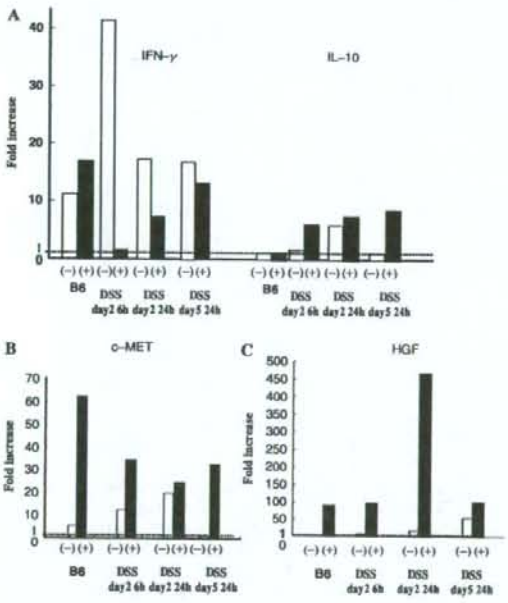

Figure 8. HGF directly regulated the expression of mRNA with decrease for IFN-γ and increase for IL-10 in *ex vivo* colonic tissue culture of mice with DSS colitis. Real-time quantitative PCR of mRNA expression for pro-inflammatory IFN-γ (A), anti-inflammatory IL-10 (A), c-Met (B), and mouse endogenous HGF (C) in the *ex vivo* colon tissue cultured with HGF. The colonic explant samples were taken from mice with DSS colitis on day 2 and day 5, or from those without DSS colitis. The explants were cultured in an organ culture dish for 6 h and 24 h. Open bars, from pCAGGS-injected mice; closed bars, pCAGGS-HGF-injected mice. Each amount was normalized to the level of GAPDH and the final relative values were expressed relative to the calibrators on day 0

Among the alternative methods, naked DNA-mediated gene transfer is the simplest, and techniques for introducing naked DNA into hepatocytes have been the most intensely studied methods for generating therapeutic amounts of gene product [23,24]. Liver-targeted gene transfer is an important tool for expanding the treatment options for diseases of several organs, as well as the liver, because the liver has a great capacity to synthesize serum proteins and is involved in numerous genetic and acquired diseases [29,30]. In this study, we used hydrodynamics-based gene transfer by tail vein injection to transfect the rat HGF gene into hepatocytes to over-express HGF in serum [31–33]. An important feature of the method is that it can achieve liver-targeted gene transfer with naked DNA that is driven by strong, non-tissue-specific, viral promoters, such as the CAG promoter [34].We could effectively transfect the HGF gene into the liver (Figure 1), and induce an ideal elevation of serum HGF levels using this method (Figures 1 and 5). Over-expression of HGF by gene transfer into the liver is an effective method for HGF production, reaching the target organ, the colon, and acting as a drug to ameliorate DSS colitis (Figure 2).

Liver-targeted gene transfer by tail vein injection has a high efficacy, but results in an accelerated decline in gene expression levels (Figure 1) compared with transfer into the muscles of mice by electroporation of the HGF gene *in vivo*. One of the mechanisms of this decline might be an immune response by the mice to the foreign protein, rat HGF. To solve this problem, we injected naked DNA twice, and succeeded in maintaining an elevated serum level of HGF (Figure 5). However, prolonged serum elevation of HGF might have unpredicted side effects on the body such as carcinogenesis [35]. Therefore, we should search for a local method of induction of naked DNA into the intestine, which could exert its therapeutic effects for the

treatment of IBD only in the colon, without increasing the serum HGF level.

This study demonstrated that (1) pretreatment with HGF gene therapy ameliorated the clinical symptoms of DSS colitis; (2) over-expressed HGF in serum ameliorated DSS colitis lesions, associated with an increase of BrdU-positive crypt epithelial cells, and decrease of apoptotic epithelial cells in the colonic crypts of DSS mice; (3) elevated serum HGF inhibited immune cell trafficking into the colon, and suppressed the pro-inflammatory response of DSS colitis; (4) these therapeutic effects of HGF depended on the duration of elevated serum HGF levels; and (5) HGF directly regulated the expressions of mRNA of IL-10 and IFN-γ in colonic explants from mice with DSS colitis.

HGF modulates intestinal epithelial proliferation and migration, serving as a critical regulator of intestinal wound healing, and several studies have reported that this growth factor is useful for the treatment of inflammatory bowel disease. Tahara *et al.* reported that administration of recombinant human HGF released by intraperitoneally transplanted osmotic pumps ameliorated DSS colitis in the rat [20]. Arthur *et al.* also reported that HGF administration by the same method ameliorated diarrhea and colitis in HLA-B27 transgenic rats [21]. Our gene therapy with HGF ameliorated DSS colitis clinically and pathologically through elevation of serum HGF (Figure 2). This could be an alternative drug-delivery method for recombinant HGF treatment of inflammatory bowel disease.

Epithelial repair is immediately accompanied by an immediate inflammatory reaction, and epithelial stem cells are induced to enter DNA synthesis as a result of wounding. HGF has been found to stimulate epithelial proliferation in the lung, stomach, and liver as well as the intestine. We have shown here that HGF gene transfer increased the numbers of BrdU-positive epithelial cells following acute DSS-induced colon injury. This might have caused rapid epithelial regeneration, as demonstrated by histological analysis showing typical regenerative changes and by higher number of surviving crypts compared with untreated mice (Figures 2 and 4).

In addition to its mitogenic activity, HGF has anti-apoptotic properties, and several reports revealed that recombinant HGF therapy ameliorated experimental colitis partially by inhibiting apoptosis of colonic epithelial cells. In this study HGF gene therapy decreased TUNEL-positive colonic epithelial cells in DSS colitis (Figure 4).

In the majority of tissues, HGF is secreted from mesenchymal cells, such as fibroblasts, and its receptor, c-Met, is found typically on epithelial cells. In our study, weak c-Met expression was observed in the crypt epithelial cells in DSS colitis, in both the pCAGGS-injected and pCAGGS-HGF-injected groups (Figure 1). Expression of c-Met mRNA was higher in the DSS colitis group injected with pCAGGS and marginal in the DSS colitis group injected with pCAGGS-HGF (unpublished observation). In the murine model of TNBS colitis, HGF gene transfer into the muscle showed an increased c-Met expression in the colon of untreated mice than those of treated mice, but phosphorylated c-Met expression was stronger in the colon of mice after HGF gene therapy than in untreated mice [36]. We are now investigating the expression of c-Met and its phosphorylation in the colons of mice with HGF gene therapy.

This study demonstrated that HGF gene therapy reduced inflammatory cell trafficking into the colon and suppressed the expression of inflammatory cytokines (Figure 3). In DSS colitis, the first insult of colonic injury is epithelial damage by DSS, resulting in destruction of the gut barrier and influx of intestinal bacterial toxins, and then the inflammatory cascade follows. HGF exerts its mitogenic and anti-apoptotic activity primarily, and thereby restores the gut barrier, leading to a reduction in the infiltration of inflammatory cells and the production of inflammatory cytokines [37,38]. Thus, the anti-inflammatory effect of HGF on DSS colitis might be the secondary effect of HGF in amelioration of DSS colitis. Interestingly, this study showed that expression of the mRNA of the anti-inflammatory cytokine IL-10 is increased markedly in mice with DSS colitis and injected with pCAGGS-HGF (Figure 3). We also observed that the numbers of IL-10-positive cells were not changed in the colons of mice with DSS colitis after HGF gene therapy (unpublished observation). These results might suggest that HGF augments the anti-inflammatory response in the inflamed colon, not by secondary effect but by its own primary effect. To address the point, we performed *ex vivo* organ culture experiments, which revealed the direct effect of HGF on immune response in the colon. We analyzed the expression of mRNA of IFN-γ and IL-10 in the colonic explants of mice with DSS colitis. In the colonic explants of mice with DSS colitis, the levels of expression of the mRNA for the pro-inflammatory cytokine IFN-γ were increased (Figure 8). The expression of mRNA for IFN-γ was clearly reduced by the treatment with HGF on explants (Figure 8), whereas expression of mRNA of IL-10 was increased markedly in the *ex vivo* colon tissue cultured with HGF (Figure 8). Thus, it is likely that HGF directly regulates the transcription of pro-inflammatory and anti-inflammatory cytokines in the diseased colonic tissue. Interestingly, the expression of mRNAs for intrinsic mouse HGF and c-Met was clearly increased in explants cultured with HGF (Figure 8).

However, the present study has not yet revealed the target cells of the HGF in the colon tissue, especially in the context of the anti-inflammatory effect of HGF. In a future study, we should identify the target cells of HGF and the molecular mechanism of how such regulation of cytokine expression works through the stimulation of c-Met, the receptor for HGF, using methods such as reporter gene expression assay.

Finally, our study showed that these therapeutic effects of HGF described above depended on the duration of elevated serum HGF level (Figures 5–7). As mentioned above, repeated injection of the HGF gene solved the problem of a short duration of response following a single injection (Figures 1 and 5). In our previous report, we

showed that repeated injection of the rat Epo gene lost its efficacy of expression of protein in the serum in rats, and the mechanism remains unclear [34]. In addition to the duration of elevated serum HGF level, Arthur *et al.* reported that there is a plateau above which a further increase in HGF levels provides no added benefit in HLA-B27 transgenic rats treated with recombinant HGF [21]. Recently, Mukoyama *et al.* reported the therapeutic effect of adenoviral-mediated HGF gene administration via the intrarectal route on TNBS-induced colitis [39]. The method could transfect the gene successfully into the epithelial cells of the colon without elevation of serum HGF levels. This could avoid the side effect of overly expressed serum HGF in serum on organs other than the intestine. On the contrary, the direct transfection of the gene into epithelial cells carries the risk of carcinogenesis of the colon [35], especially considering the chronic intestinal inflammatory status of patients with inflammatory bowel disease. We must be cautious when choosing the best method for HGF gene transfer, to enable HGF to work maximally in the target organ of the intestine.

In conclusion, this study demonstrated that hydrodynamics-based transfection of the rat HGF gene into the liver via tail vein injection ameliorated DSS colitis in mice, and its effect appears to depend on the duration of elevated serum HGF level. These results suggest that HGF gene therapy could be a new therapeutic approach to inflammatory bowel disease.

Acknowledgements

We thank Norio Honda and Takao Tsuchida for technical assistance and Dr. Minoru Nomoto, Dr. Terasu Honma, and Dr. Yasunobu Matsuda for helpful discussions. We also thank Dr. Suresh S. Palaniyandi for editing the English in the manuscript. This work was supported by grants from the Ministry of Health, Welfare, and Labor of the Government of Japan.

References

1. Podolsky DK. Inflammatory bowel disease. *N Engl J Med* 2002; **347**: 417–429.
2. Sands BE. Therapy of inflammatory bowel disease. *Gastroenterology* 2000; **118**: S68–S82.
3. Shanahan F. Inflammatory bowel disease: immunodiagnostics, immunotherapeutics, and ecotherapeutics. *Gastroenterology* 2001; **120**: 622–635.
4. Sandborn WJ, Targan SR. Biologic therapy of inflammatory bowel disease. *Gastroenterology* 2002; **122**: 1592–1608.
5. Targan SR, Hanauer Sb, van Deventer SJ, *et al.* A short-term study of chimeric monoclonal antibody cA2 to tumor necrosis factor alpha for Crohn's disease. Crohn's Disease cA2 Study Group. *N Engl J Med* 1997; **337**: 1029–1035.
6. Ito H, Takazoe M, Fukuda Y, *et al.* A pilot randomized trial of a human anti-interleukin-6 receptor monoclonal antibody in active Crohn's disease. *Gastroenterology* 2004; **126**: 989–996.
7. Playford RJ. Peptides and gastrointestinal mucosal integrity. *Gut* 1995; **37**: 595–597.
8. Procaccino F, Reinshagen M, Hoffmann P, *et al.* Protective effect of epidermal growth factor in an experimental model of colitis in rats. *Gastroenterology* 1994; **107**: 12–17.
9. Sinha A, Nightingale JMD, West KP, *et al.* Epidermal growth factor enemas with oral mesalamine for mild-to-moderate left-sided ulcerative colitis. *N Engl J Med* 2003; **349**: 350–357.
10. Boros P, Miller CM. Hepatocyte growth factor: a multifunctional cytokine. *Lancet* 1995; **345**: 293–295.
11. Zarnegar R, Michalopoulos GK. The many faces of hepatocyte growth factor: from heptopoiesis to hematopoiesis. *J Cell Biol* 1995; **129**: 1177–1180.
12. Nakamura T, Nishizawa T, Hagiya M, *et al.* Molecular cloning and expression of human hepatocyte growth factor. *Nature* 1989; **342**: 440–443.
13. Nishimura S, Takahashi M, Ota S, *et al.* Hepatocyte growth factor accelerates restitution of intestinal epithelial cells. *J Gastroenerol* 1998; **33**: 172–178.
14. Tsuji S, Kawano S, Tsujii M, *et al.* Roles of hepatocyte growth factor and its receptor in gastric mucosa. A cell biological and molecular biological study. *Dig Dis Sci* 1995; **40**: 1132–1139.
15. Nusrat A, Parkos CA, Bacarra AE, *et al.* Hepatocyte growth factor/scatter factor effects on epithelia. Regulation of intercellular junctions in transformed and nontransformed cell lines, basolateral polarization of c-met receptor in transformed and natural intestinal epithelia, and induction of rapid wound repair in a transformed model epithelium. *J Clin Invest* 1994; **93**: 2056–2065.
16. Bottaro DP, Rubin JS, Faletto DL, *et al.* Identification of the hepatocyte growth factor receptor as the c-met proto-oncogene product. *Science* 1991; **251**: 802–804.
17. Itoh H, Naganuma S, Takeda N, *et al.* Regeneration of injured intestinal mucosa is impaired in hepatocyte growth factor activator-deficient mice. *Gastroenterology* 2004; **127**: 1423–1435.
18. Kitamura S, Kondo S, Shinomura Y, *et al.* Expression of heptocyte growth factor and c-met in ulcerative colitis. *Inflamm Res* 2000; **49**: 320–324.
19. Ortega-Cava CF, Ishihara S, Kawashima K, *et al.* Hepatocyte growth factor expression in dextran sodium sulfate-induced colitis in rats. *Dig Dis Sci* 2002; **47**: 2275–2285.
20. Tahara Y, Ido A, Yamamoto S, *et al.* Hepatocyte growth factor facilitates colonic mucosal repair in experimental ulcerative colitis in rats. *J Pharmacol Exp Ther* 2003; **307**: 146–151.
21. Arthur G, Schwartz MZ, Kuenzler KA, Birbe R. Hepatocyte growth factor treatment ameliorates diarrhea and bowel inflammation in a rat model of inflammatory bowel disease. *J Pediatr Surg* 2004; **39**: 139–143.
22. Hickman MA, Malone RW, Lehmann-Bruinsma K, *et al.* Gene expression following direct injection of DNA into liver. *Hum Gene Ther* 1994; **5**: 1477–1483.
23. Paillard F. Naked DNA gene delivery to the liver. *Hum Gene Ther* 1997; **8**: 1735–1736.
24. Liu F, Song Y, Liu D. Hydrodynamics-based transfection in animals by systemic administration of plasmid DNA. *Gene Ther* 1999; **6**: 1258–1266.
25. Sasaki S, Yoneyama H, Suzuki K, *et al.* Blockade of CXCL10 protects mice from acute colitis and enhances crypt cell survival. *Eur J Immunol* 2002; **32**: 3197–3205.
26. M Noguchi, N Hiwatashi, Z Liu, T Toyota. Secretion imbalance between tumor necrosis factor and its inhibitor in inflammatory bowel disease. *Gut* 1998; **43**: 203–209.
27. Hacein-Bey-Abina S, von Kalle C, Schmidt M, *et al.* A serious adverse event after successful gene therapy for X-linked severe combined immunodeficiency. *N Engl J Med* 2003; **348**: 255–256.
28. Hacein-Bey-Abina S, Von Kalle C, Schmidt M, *et al.* LMO2-associated clonal T cell proliferations in two patients after gene therapy for SCID-X1. *Science* 2003; **302**: 415–419.
29. Ueki T, Kaneda Y, Tsutsui H, *et al.* Hepatocyte growth factor gene therapy of liver cirrhosis in rats. *Nat Med* 1999; **5**: 226–230.
30. Kuroiwa T, Kakishita E, Hamano T, *et al.* Hepatocyte growth factor ameliorates acute graft-versus-host disease and promotes hematopoietic function. *J Clin Invest* 2001; **107**: 1365–1373.
31. Zhang G, Budker V, Wolff JA. High levels of foreign gene expression in hepatocytes after tail vein injections of naked plasmid DNA. *Hum Gene Ther* 1999; **10**: 1735–1737.
32. Zhang G, Song YK, Liu D. Long-term expression of human alpha1-antitrypsin gene in mouse liver achieved by intravenous administration of plasmid DNA using a hydrodynamics-based procedure. *Gene Ther* 2000; **7**: 1344–1349.
33. Miao CH, Thompson AR, Loeb K, *et al.* Long-term and therapeutic-level hepatic gene expression of human factor IX after naked plasmid transfer in vivo. *Mol Ther* 2001; **3**: 947–957.

34. Maruyama H, Higuchi N, Nishikawa Y, *et al.* High-level expression of naked DNA delivered to rat liver via tail vein injection. *J Gene Med* 2002; **4**: 333–341.
35. Takayama H, LaRochelle WJ, Sharp R, *et al.* Diverse tumorigenesis associated with aberrant development in mice overexpressing hepatocyte growth factor/scatter factor. *Proc Natl Acad Sci U S A* 1997; **94**: 701–706.
36. Oh K, Iimuro Y, Takeuchi M, *et al.* Ameliorating effect of hepatocyte growth factor on inflammatory bowel disease in a murine model. *Am J Physiol* 2004; **288**: 729–735.
37. Okayasu I, Hatakeyama S, Ohkusa T, Inagaki Y, Nakaya R. A novel method in the induction of reliable experimental acute and chronic ulcerative colitis in mice. *Gastroenterology* 1990; **98**: 694–702.
38. Cooper HS, Murthy SN, Shah RS, Sedergran DJ. Clinicopathologic study of dextran sulfate sodium experimental murine colitis. *Lab Invest* 1993; **69**: 238–249.
39. Mukoyama T, Kanbe T, Murai R, *et al.* Therapeutic effect of adenoviral-mediated hepatocyte growth factor gene administration on TNBS-induced colitis in mice. *Biochem Biophys Res Commun* 2005; **329**: 1217–1224.

Role of IP-10/CXCL10 in the progression of pancreatitis-like injury in mice after murine retroviral infection

Yusuke Kawauchi, Kenji Suzuki, Shiro Watanabe, Satoshi Yamagiwa, Hiroyuki Yoneyama, Gi Dong Han, Suresh S. Palaniyandi, Punniyakoti T. Veeraveedu, Kenichi Watanabe, Hiroshi Kawachi, Yoshiaki Okada, Fujio Shimizu, Hitoshi Asakura, Yutaka Aoyagi and Shosaku Narumi

Am J Physiol Gastrointest Liver Physiol 291:345-354, 2006. doi:10.1152/ajpgi.00002.2006

Am J Physiol Gastrointest Liver Physiol 291: G345–G354, 2006;
doi:10.1152/ajpgi.00002.2006.

Role of IP-10/CXCL10 in the progression of pancreatitis-like injury in mice after murine retroviral infection

Yusuke Kawauchi,[1] Kenji Suzuki,[1] Shiro Watanabe,[1] Satoshi Yamagiwa,[1] Hiroyuki Yoneyama,[2] Gi Dong Han,[3,6] Suresh S. Palaniyandi,[4] Punniyakoti T. Veeraveedu,[4] Kenichi Watanabe,[4] Hiroshi Kawachi,[3] Yoshiaki Okada,[5] Fujio Shimizu,[3] Hitoshi Asakura,[1] Yutaka Aoyagi,[1] and Shosaku Narumi[2]

Departments of [1]Gastroenterology and Hepatology and [3]Cell Biology, Institute of Nephrology, Niigata University Graduate School of Medical and Dental Sciences, Niigata; [5]Department of Bacterial and Blood Products, National Institute of Infectious Diseases, Tokyo; [2]Department of Molecular Preventive Medicine, University of Tokyo Graduate School of Medicine, Tokyo; [4]Department of Clinical Pharmacology, Niigata University of Pharmacy and Applied Life Sciences, Niigata, Japan; and [6]Department of Food Science and Technology, Yeungnam University, Gyeongsan, Republic of Korea

Submitted 4 January 2006; accepted in final form 1 April 2006

Kawauchi, Yusuke, Kenji Suzuki, Shiro Watanabe, Satoshi Yamagiwa, Hiroyuki Yoneyama, Gi Dong Han, Suresh S. Palaniyandi, Punniyakoti T. Veeraveedu, Kenichi Watanabe, Hiroshi Kawachi, Yoshiaki Okada, Fujio Shimizu, Hitoshi Asakura, Yutaka Aoyagi, and Shosaku Narumi. Role of IP-10/CXCL10 in the progression of pancreatitis-like injury in mice after murine retroviral infection. *Am J Physiol Gastrointest Liver Physiol* 291: G345–G354, 2006; doi:10.1152/ajpgi.00002.2006.—Exocrinopathy and pancreatitis-like injury were developed in C57BL/6 (B6) mice infected with LP-BM5 murine leukemia virus, which is known to induce murine acquired immunodeficiency syndrome (MAIDS). The role of chemokines, especially CXCL10/interferon (IFN)-γ-inducible protein 10 (IP-10), a chemokine to attract CXCR3$^+$ T helper 1-type CD4$^+$ T cells, has not been investigated thoroughly in the pathogenesis of pancreatitis. B6 mice were inoculated intraperitoneally with LP-BM5 and then injected every week with either an antibody against IP-10 or a control antibody. Eight weeks after infection, we analyzed the effect of IP-10 neutralization. Anti-IP-10 antibody treatment did not change the generalized lymphadenopathy and hepatosplenomegaly of mice with MAIDS. The treatment significantly reduced the number of IP-10- and CXCR3-positive cells in the mesenteric lymph nodes (mLNs) but not the phenotypes and gross numbers of cells. In contrast, IP-10 neutralization reduced the number of mononuclear cells infiltrating into the pancreas. Anti-IP-10 antibody treatment did not change the numbers of IFN-γ$^+$ and IL10$^+$ cells in the mLN but significantly reduced their numbers, especially IFN-γ$^+$ and IL-10$^+$ CD4$^+$ T cells and IFN-γ$^+$ Mac-1$^+$ cells, in the pancreas. IP-10 neutralization ameliorated the pancreatic lesions of mice with MAIDS probably by blocking the cellular infiltration of CD4$^+$ T cells and IFN-γ$^+$ Mac-1$^+$ cells into the pancreas at least at 8 wk after infection, suggesting that IP-10 and these cells might play a key role in the development of chronic autoimmune pancreatitis.

autoimmune pancreatitis; Sjögren's syndrome; murine acquired immodeficiency syndrome; chemokines; interferon-γ-inducible protein 10

CHEMOKINES, which are chemotactic cytokines, control the essential process of the attraction of leukocytes to the tissues in inflammation (1, 18). The chemokine family comprises two major subfamilies, termed CXC and CC according to the arrangement of the first two conserved cysteines, which are separated by one amino acid and are adjacent, respectively (1, 18). Interferon (IFN)-γ-inducible protein of 10 kDa (IP-10/CXCL10) is a member of the CXC chemokine family and a potent chemoattractant for activated T lymphocytes, natural killer cells, and monocytes (6, 17). It is also considered as a regulator of T helper (Th)1 inflammatory responses (26). The expression of IP-10 was elevated in several diseases such as ulcerative colitis (34), hepatitis (21), multiple sclerosis (31), and Sjögren's syndrome (SjS) (22), suggesting the involvement of IP-10 in the development of these diseases. It has been recently reported that IP-10 is expressed by β-cells of the islets of Langerhans, resulting in the preferential accumulation of CXCR3$^+$ T cells into the pancreas in a virus-induced Type I diabetic mouse model (7). Information about the role of chemokines in pancreatic diseases, however, is limited and needs further investigation (2, 28). In the pathogenesis of chronic pancreatitis, especially with autoimmune etiology, the role of chemokines such as IP-10 has not been investigated thoroughly.

The LP-BM5 murine leukemia virus (MuLV) is a retrovirus that is known to induce profound immunodeficiency with splenomegaly and generalized lymphadenopathy in susceptible strains of mice, such as C57BL/6 (B6) mice, and occasionally brings about lymphoid malignancy (10, 14, 19). In the early phase of infection, hypergammaglobulinemia and polyclonal B and T cell activation are induced and autoantibodies such as anti-nuclear and anti-double-stranded DNA antibodies are detected in mice infected with the virus (10, 14, 19). In the late phase of infection, virus-infected B6 mice show symptoms similar to those of human acquired immunodeficiency syndrome (AIDS); therefore, they have been studied as a murine model of AIDS, termed as murine AIDS (MAIDS) (10, 14, 19). We have reported previously that systemic exocrinopathy resembling SjS was induced in systemic exocrine glands such as salivary glands and lachrymal glands and in the pancreas of virus-infected mice; thus we proposed that mice with MAIDS could be an animal model for SjS as well as AIDS (32, 33). In mice with MAIDS, the pancreatic lesions are the exocrine system-oriented inflammation characterized by cellular infil-

Address for reprint requests and other correspondence: K. Suzuki, Dept. of Gastroenterology and Hepatology, Niigata Univ. Graduate School of Medical and Dental Sciences, 1-757 Asahimachi-dori, Niigata 951-8510, Japan (e-mail: kjsuzuki@med.niigata-u.ac.jp).

The costs of publication of this article were defrayed in part by the payment of page charges. The article must therefore be hereby marked "*advertisement*" in accordance with 18 U.S.C. Section 1734 solely to indicate this fact.

tration around the interlobular pancreatic ducts and acinar cell destruction (32, 33, 35), but with no damage of the endocrine system, that is, the islets of Langerhans (35). The pancreas-infiltrating cells comprise both Th1- and Th2-type $CD4^+$ T cells, although with a predominance of Th2 cells over Th1 cells (35). Thus the pancreatic lesions of the mice have some similarities to autoimmune-related chronic pancreatitis, especially the lesions associated with SjS.

To clarify the role of IP-10 in the development of chronic pancreatitis with autoimmune etiology, especially associated with SjS, we investigated the effect of CXCL10 neutralization on pancreatic lesions of mice with MAIDS. Our results suggest that anti-IP-10 monoclonal antibody ameliorated the pancreatic lesions of mice with MAIDS.

MATERIALS AND METHODS

Animals. Four-week-old female B6 mice were purchased from Charles River Japan (Kanagawa, Japan) and maintained at the Animal Center of the Niigata University School of Medicine under specific-pathogen-free conditions. All animal experiments were performed according to the "Guide for Animal Experiments" of Niigata University School of Medicine.

Induction of MAIDS. LP-BM5 MuLV was prepared from the supernatant of cloned G6 cells infected with the retrovirus as reported previously (35). Four-week-old B6 female mice were injected intraperitoneally with 0.3 ml of LP-BM5 MuLV virus stock solution. At 8 wk after virus inoculation, mice with MAIDS were killed by cervical dislocation under ether anesthesia, and their pancreases were removed for further analysis. For blocking experiments, PBS containing 100 μg/100 μl anti-CXCL10 monoclonal antibodies (36) or anti-human parathyroid-related peptide monoclonal antibodies, which was the IgG_1 subclass-matched control monoclonal antibody, or PBS alone were administered intraperitoneally at the time of virus inoculation and once a week thereafter.

Monoclonal antibodies. For immunofluorescence (IF) and flow cytometric analyses, the following monoclonal antibodies were used: anti-CD4 (clone GK1.5, IgG_{2b}), anti-CD8 (clone 53-6.7, IgG_{2a}), anti-B220 (clone RA3-6B2, IgG_{2a}), anti-Mac-1 (clone M-70.15, IgG_{2b}), anti-mouse INF-γ (clone XMG1.2), and anti-mouse IL-10 (clone JES5-16E3). For immunostaining of IP-10 or CXCR3, goat polyclonal antibodies to IP-10 or CXCR3 (Santa Cruz Biotechnology; Santa Cruz, CA) were used.

Detection of LP-BM5 MuLV by PCR. The PCR method used for the detection of the virus was as reported previously (33).

Quantitative RT-PCR to detect cytokine mRNA. Total RNA was extracted from the mesenteric lymph node (mLN) and pancreas specimens with TRIzol (GIBCO-BRL) according to the standard protocol and reverse transcribed. Thereafter, cDNA was amplified using the ABI 7700 sequence detector system (Applied Biosystems; Foster City, CA) with a set of primers and probes corresponding to IFN-γ, IL-10, IP-10, CXCR3, and GAPDH as previously described (36).

Histopathological examination. Tissue samples were taken from the pancreas, fixed in 10% buffered formalin, and then embedded in paraffin wax blocks. Sections (4-μm thick) were made in the usual way and stained with hematoxylin and eosin. The stained sections were then examined by light microscopy.

The numbers of inflammatory cells in a high-power field (×400) were counted under a microscope, and the degree of pancreatitis was assessed from *0* to *4* as reported previously (11, 24).

IF staining procedure. Frozen sections of the pancreas were prepared in a cryostat and stained with several fluorescent dye-conjugated anti-mouse antibodies as described above. The sections were observed by fluorescence microscopy.

Double-IF staining procedure. For the simultaneous demonstration of cell surface antigens and cytokines, the IF staining method was as reported previously (35).

Statistical analysis. Data are expressed as means ± SD. Statistical analyses were performed using the unpaired Student's *t*-test or the nonparametric Mann-Whitney test. Differences were considered significant at $P < 0.05$.

RESULTS

IP-10 neutralization did not prevent infection by the MAIDS virus. All mice infected with LP-BM5 MuLV developed characteristic MAIDS symptoms such as generalized lymphadenopathy and hepatosplenomegaly ($n = 15$), and neutralization of IP-10 did not change the course of MAIDS ($n = 15$). Eight weeks after the virus inoculation, there were no differences in the weights of the liver, spleen, and mLNs between mice with MAIDS injected with anti-IP-10 monoclonal antibody and those injected with control antibody (Fig. 1*A*). A defective LP-BM5 virus genome was detected in mice of both groups by

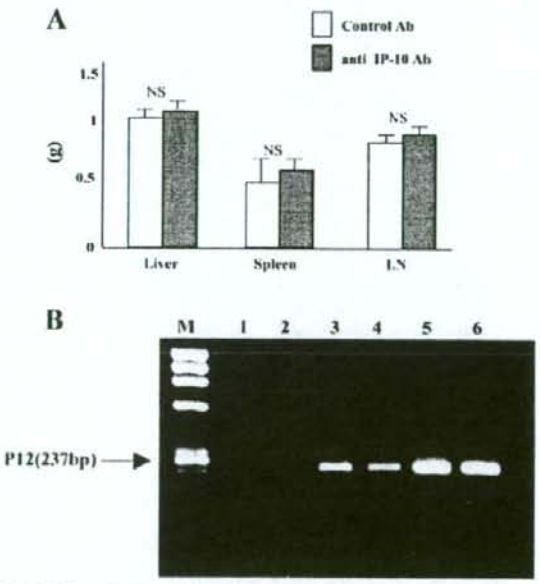

Fig. 1. Effect of neutralization of interferon (IFN)-γ-inducible protein of 10 kDa (IP-10/CXCL10) on the course of murine acquired immunodeficiency syndrome (MAIDS). *A*: effect of neutralization of IP-10 on organs of mice with MAIDS. The weights of the liver, spleen, and mesenteric lymph nodes (LNs) of mice with MAIDS injected with control antibody (Ab) were increased at 8 wk after infection. However, they were not changed after the injection of anti-IP-10 monoclonal (m)Ab. Data are means ± SD. NS, not significant. *B*: neutralization of IP-10 did not prevent infection by the MAIDS virus. LP-BM5 murine leukemia virus (MuLV) was detected in the mesenteric LNs and pancreas of mice with MAIDS at 8 wk after infection. Template DNAs were extracted from frozen sections of the pancreas and then analyzed by PCR with P12 primer. The bands were obtained by running the PCR products in agarose gel. M, molecular size marker; *lane 1*, the mesenteric LN of an uninfected C57BL/6 (B6) mouse (negative control); *lane 2*, the pancreas of an uninfected B6 mice (negative control); *lane 3*, the mesenteric LN of a mouse with MAIDS injected with control Ab; *lane 4*, the pancreas of a mouse with MAIDS injected with control Ab; *lane 5*, the mesenteric LN of a mouse with MAIDS injected with anti-IP-10 mAb; *lane 6*, the pancreas of a mouse with MAIDS injected with anti-IP-10 mAb.

PCR in the same frozen sections of the mLNs and pancreas of mice with MAIDS as those used for immunohistochemical staining (Fig. 1*B*). P12 of the virus genome was not detected in untreated normal B6 mice (Fig. 1*B*).

Effect of IP-10 neutralization on the expression of IP-10 and CXCR3 by lymphoid cells in mice with MAIDS. In the mLN and pancreas of mice with MAIDS injected with control antibody, the expression levels of mRNA for IP-10 and its receptor CXCR3 were significantly increased compared with untreated B6 mice (Fig. 2*A*). Neutralization of IP-10 down-regulated the expression of mRNA for IP-10 and CXCR3 in the mLNs and pancreas of mice with MAIDS (Fig. 2, *A* and *B*). Next, we analyzed their expressions in the pancreas and mLN by IF. In normal mice, IP-10 and CXCR3 were detected neither in the mLN nor in the pancreas, with the exception of a few $CXCR3^+$ cells scattered in the mLN (data not shown). The numbers of cells that expressed IP-10 and CXCR3 increased in the mLN and pancreas of mice with MAIDS injected with control antibody (Fig. 3*I*, *A* and *B*, and *II*, *A* and *B*). Double-color IF revealed that in the mLN, some $IP\text{-}10^+$ cells were $Mac\text{-}1^+$ cells and $CXCR3^+$ cells were mainly $CD4^+$ T cells (Fig. 3*I*, *C* and *D*). In the pancreas of mice with MAIDS, IP-10 and CXCR3 were mainly detected on some cells in an inflammatory cell focus around the pancreatic duct (Fig. 3*II*, *A* and *B*). Double-color IF showed that $IP\text{-}10^+$ cells were not positive for CD4, CD8, B220, and Mac-1 (Fig. 3*II*, *C*). It also revealed that $CXCR3^+$ cells were mainly $CD4^+$ T cells (Fig. 3*II*, *D*). Interestingly, IP-10 was also detected on some cells localized between the basal laminas that envelope each acinus of a minimal functional unit of the exocrine system of the pancreas (Fig. 3*II*, *A*, *inset*). Neutralization of IP-10 decreased the numbers of cells that expressed IP-10 or CXCR3 in the mLN (Fig. 3*I*, *E* and *F*) and pancreas (Fig. 3*II*, *E* and *F*) of mice with MAIDS.

Effect of IP-10 neutralization on mLN cells of mice with MAIDS. IF study of the mLN revealed that the numbers of $CD4^+$, $CD8^+$, $B220^+$, and $Mac\text{-}1^+$ cells were unchanged statistically by neutralization of IP-10 (Fig. 4*A*).

To reveal the systemic effect of IP-10 neutralization on cytokine production, we analyzed the number of IFN-γ- and IL-10-positive cells in the mLN of mice with MAIDS at 8 wk after infection by IF. We chose IFN-γ as a representative for a proinflammatory cytokine (or Th1 response) and IL-10 as a representative of an anti-inflammatory cytokine (or Th2). In mLNs of mice with MAIDS, there was no significant difference between the anti-IP-10 monoclonal antibody-treated group and the control antibody-treated group in IL-10- and IFN-γ-positive cells (Fig. 4*B*). IP-10 neutralization did not change the number of these cytokine-positive cells in the mLN of mice with MAIDS (Fig. 4*B*).

IP-10 neutralization ameliorated pancreatic lesions of mice with MAIDS. We have previously reported that periductal mononuclear cellular infiltration resembling autoimmune pancreatitis associated with SjS was detected in mice with MAIDS

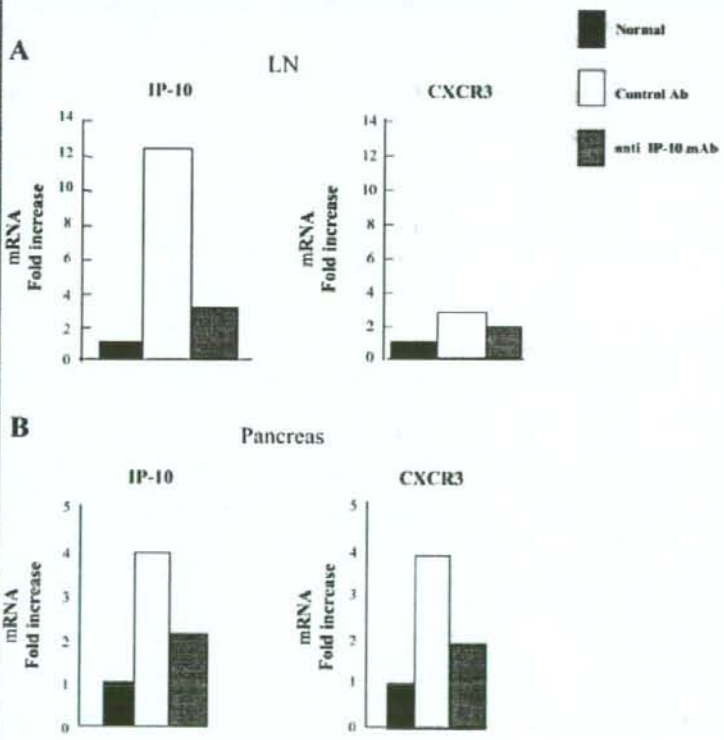

Fig. 2. Real-time quantitative PCR analysis of IP-10 and CXCR3 mRNA expression. The expressions of IP-10 and CXCR3 mRNA of the mesenteric LNs (*A*) and pancreas (*B*) were analyzed. Each amount was normalized to the level of each GAPDH. Final relative values are expressed relative to the calibrators (Ref. 36) as described above.

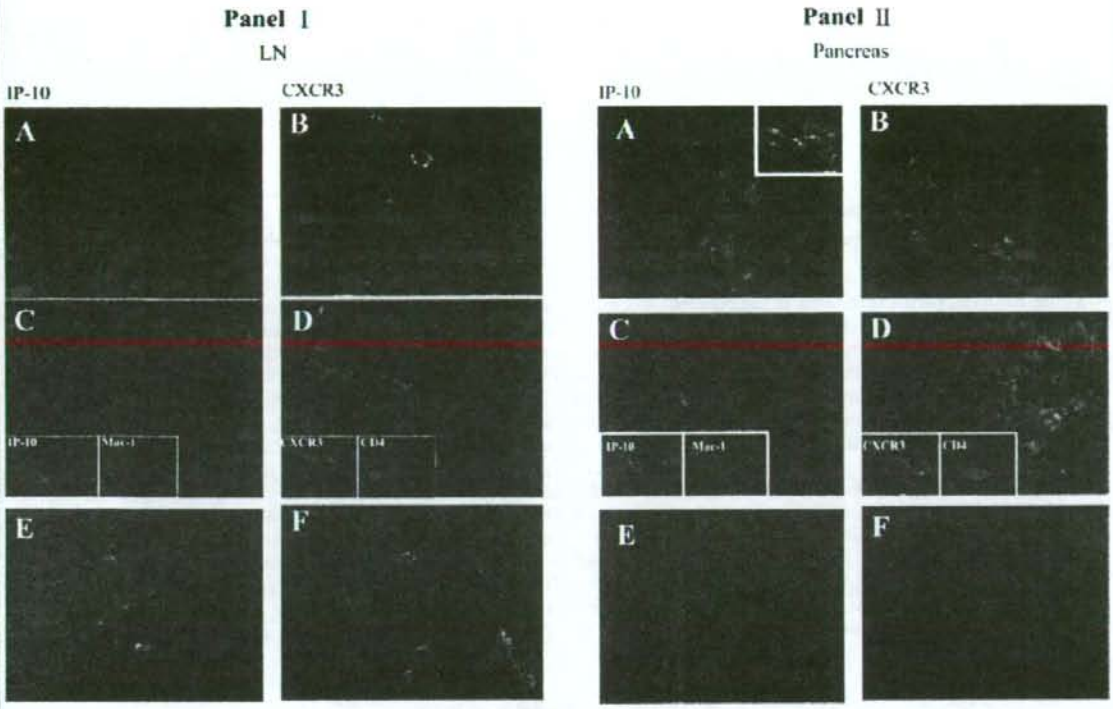

Fig. 3. *I*: effect of neutralization of IP-10/CXCL10 on the expressions of IP-10 and CXCR3 in the mesenteric LNs of mice with MAIDS. IP-10- and CXCR3-positive cells were detected in the mesenteric LNs of mice with MAIDS injected with control Ab (*A* and *B*). Their numbers decreased in the mesenteric LNs of mice with MAIDS injected with anti-IP-10 mAb (*E* and *F*). Some of the IP-10$^+$ cells (green) were Mac-1$^+$ cells (red), but were never positive for CD4, CD8, or B220 (*C*). Most of the CXCR3$^+$ cells (green) were positive for CD4 (red) (*D*). IP-10 was not detected, but CXCR3 was detected on a few cells in the mesenteric LN of an untreated B6 mouse (data not shown). *A*, *C*, and *E*, anti-IP-10 mAb-stained sections; *B*, *D*, and *F*, other sections stained with anti-CXCR3 Ab. *II*: effect of neutralization of IP-10 on the expressions of IP-10 and CXCR3 in the pancreas of mice with MAIDS. IP-10-and CXCR3-positive cells were detected in the pancreas of mice with MAIDS injected with control Ab (*A* and *B*). In the pancreas of mice with MAIDS, IP-10 and CXCR3 were mainly detected on some cells in a inflammatory cell focus around a pancreatic duct (*A* and *B*). Interestingly, IP-10 was also detected on cells localized between basal laminas that envelope each acinus of a minimal functional unit of the exocrine system of the pancreas (*A*, *inset*). IP-10$^+$ cells (green) were not positive for Mac-1$^+$ cells (red), CD4, CD8, or B220 (*C*). Most of the CXCR3$^+$ cells (green) were positive for CD4 (red) (*D*). IP-10 was not detected, but CXCR3 was detected on a few cells in the mesenteric LN of an untreated B6 mouse (data not shown). IP-10-and CXCR3-positive cells were not detected in the pancreas of mice with MAIDS injected with anti-IP-10 mAb (*E* and *F*). IP-10 and CXCR3 were not detected in the pancreas of an untreated B6 mouse (*A* and *B*). *A*, *C*, and *E*, sections stained with anti-IP-10 mAb; *B*, *D*, and *F*, sections stained with anti-CXCR3 Ab.

and the numbers of infiltrating cells and the grades of the lesions reached a peak at 8 wk after infection. To evaluate the effect of IP-10 neutralization, we, therefore, analyzed the pancreatic lesions of mice with MAIDS at 8 wk after infection. In mice with MAIDS injected with control antibody, inflammatory cells were detected around the pancreatic ducts, from where they progressively expanded, pressing the acinar architecture outward (Fig. 5*A*). At the interface lesions between the infiltrating cells and pancreatic parenchyma, destructed acinar cells were detected, but the degree of acinar cell destruction by infiltrating cells was rather mild (Fig. 5*C*). Peri-islet cellular infiltration was also observed (Fig. 5, *A* and *C*). Anti-IP-10 monoclonal antibody treatment clearly ameliorated the pathological lesions of the pancreas of mice with MAIDS (Fig. 5, *B* and *D*); the size of periductal cellular infiltration became smaller and the numbers of destructed acinar cells were also decreased (Fig. 5, *B* and *D*). Both the numbers of pancreas-infiltrating cells and the histological grading scores of the pancreatitis were significantly reduced by IP-10 neutralization (Fig. 5, *E* and *F*).

IP-10 neutralization ameliorated pancreatic lesions through decreased migration of CD4$^+$T, Mac-1$^+$, and B220$^+$ cells in mice with MAIDS. Eight weeks after infection, pancreas-infiltrating cells were composed of CD4$^+$ and CD8$^+$ T cells, Mac-1$^+$ macrophages, and B220$^+$ B cells but not natural killer cells or granulocytes. The major populations of infiltrating cells were composed CD4$^+$ T cells, Mac-1$^+$ macrophages, and B220$^+$ cells (Fig. 6, *A*, *C*, *E*, and *G*). The IF study showed that IP-10 neutralization significantly decreased the numbers of CD4$^+$ T, Mac-1$^+$, and B220$^+$ cells in pancreatic lesions of mice with MAIDS (Fig. 6, *B*, *D*, *F*, and *G*).

IP-10 neutralization decreased the migration of IFN-γ- and IL-10-producing CD4$^+$T and Mac-1$^+$ cells in the pancreas of mice with MAIDS. To reveal the effect of IP-10 neutralization on the immune response in the pancreas of mice with MAIDS, we analyzed the cytokine expression of IFN-γ and IL-10. The

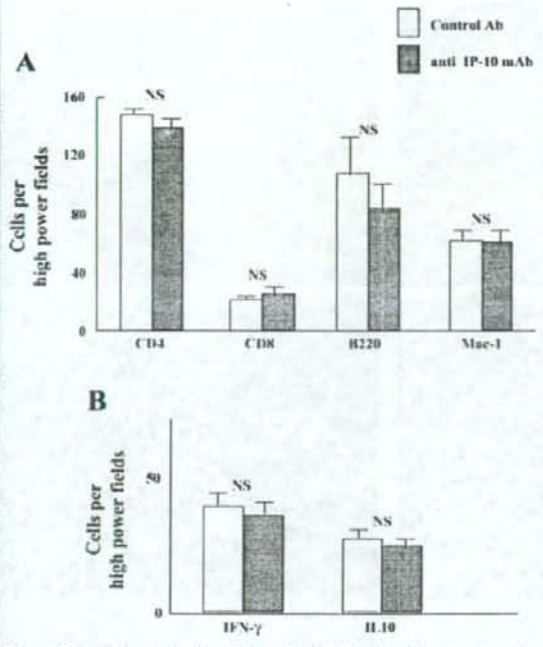

Fig. 4. Effect of neutralization of IP-10/CXCL10 on lymphocyte subpopulations in the LNs of mice with MAIDS. *A*: quantitative analysis of immune cells in the LNs by immunofluorescence (IF) for CD4, CD8, Mac-1, and B220. *B*: quantitative analysis of IFN-γ and IL-10 expression in the mesenteric LNs of mice with MAIDS at 8 wk after infection. Each focus of cellular infiltration was examined for the presence of CD4, CD8, B220, Mac-1, IFN-γ, and IL-10 cells. Final results are presented as the numbers of cells per high-powered microscope field. Representative findings (means ± SD; $n = 10$) from 3 independent experiments are shown.

levels of expression of the mRNAs of both cytokines in the pancreas were significantly increased after infection, and IP-10 neutralization decreased them (Fig. 7*A*). IF showed that IP-10 neutralization significantly decreased the numbers of IFN-γ- and IL-10-positive cells in the pancreas of mice with MAIDS (Fig. 7*B*).

Next, by the double-color IF method, we characterized the phenotypes of cells producing these cytokines. IFN-γ and IL-10 were mainly present on $CD4^+$ T cells (Fig. 8, *A* and *C*) and Mac-1^+ cells (Fig. 8, *E* and *G*) but not on $B220^+$ cells or $CD8^+$ T cells (data not shown). We did not detect the expression of IFN-γ or IL-10 in the pancreas of normal B6 mice (data not shown).

The numbers of IFN-γ- and IL-10-positive $CD4^+$ T cells were significantly reduced in mice with MAIDS by IP-10 neutralization (Figs. 7*C* and 8, *B* and D). Additionally, IP-10 neutralization significantly reduced the numbers of IFN-γ-positive Mac-1^+ cells in the pancreas of mice with MAIDS (Figs. 7*D* and 8*F*). The numbers of IL-10-positive Mac-1^+ cells became smaller by IP-10 neutralization, but there was no statistical significance between the mice with or without treatment (Figs. 7*D* and 8, *G* and *H*).

DISCUSSION

We have shown that systemic exocrinopathy including exocrine pancreatitis-like injury developed concordantly with the progression of MAIDS symptoms. Therefore, exocrine pancreatitis-like injury of mice with MAIDS might be a manifestation of several characteristic symptoms of MAIDS such as hepatomegaly, splenomegaly, systemic lymphadenopathy, and abnormal immunological reactions. In this study, we have shown that IP-10 neutralization ameliorated the pancreatic lesions of mice with MAIDS (Fig. 5) but prevented neither the infection nor the course of MAIDS (Fig. 1). These results suggest a different mechanism for the pathogenesis of systemic exocrinopathy including exocrine pancreatitis-like injury of MAIDS and the other MAIDS symptoms.

In the *Toxoplasma gondii* infection model, IP-10 neutralization inhibited the accumulation of effector T cells, resulting in a decreased ability to kill the parasite in target organs such as the liver, spleen, brain, and lung (12). IP-10 neutralization studies and a study on IP-$10^{-/-}$ mice also showed that the blockade of effector cell trafficking resulted in the breakdown of host defenses in neurotropic mouse hepatitis virus infection in the brain (5, 16). In the liver of patients with chronic active hepatitis C, we (21) have reported that IP-10 mRNA was expressed mainly in hepatocytes around intralobular focal and periportal piecemeal necrosis. These examples suggest that if the organ of the specific lesions induced by a particular infection was the same as the target organ of the infectious agent, IP-10 neutralization could ameliorate the organ lesions by inhibiting the trafficking of effector cells that eliminate the infectious agents from the target organ. In MAIDS, we reported previously that the virus was integrated in Ly-1 B cells but not in T cells (9) or on parenchymal cells of the pancreas (unpublished observations), although several reports have shown that B cells (13) and macrophages (4) as well as T cells (15) can serve as targets for infection of the virus. Therefore, pancreatic tissues are not the direct target cells of LP-BM5 infection, and the IP-10 neutralization-induced amelioration of pancreatic lesions of MAIDS cannot be explained by the decreased accumulation of effector cells that eliminate LP-BM5 from the pancreas.

We and others have reported that systemic exocrinopathy including pancreatitis-like injury is the characteristic organ lesions of mice with MAIDS (10, 14, 19, 32, 33, 35); however, the target antigen in exocrine glands, which regulates the target organ specificity, has been unknown. Without knowing the target antigen, delineating the process of inflammatory cell infiltration provides a basis for understanding the development of the pancreatic lesions of MAIDS. The blocking activity of the anti-IP-10 monoclonal antibody used in this study was confirmed in the chemotactic assay and in some other murine models depicting acute colitis (27) and encephalomyelitis (20). We confirmed that the anti-IP-10 monoclonal antibody had no cross-reactivity with other chemokines such as the monokine induced by IFN-γ, macrophage inflammatory protein-1α, or mature dendritic cells (36). In this study, therefore, we examined the expression of IP-10 and its receptor CXCR3 in the mLN and pancreas of mice with MAIDS. In the mLN and pancreas of MAIDS, IP-10 was mainly expressed on Mac-1^+ cells and CXCR3 was mainly detected on $CD4^+$ T cells. Anti-IP-10 treatment clearly reduced the number of these cells in both the mLN and pancreas. Our results suggest that cell trafficking into the pancreas of mice with MAIDS is carried out by the interaction between IP-10 and CXCR3 of $CD4^+$ cells. In the virus-induced Type I diabetes mouse model, it has been

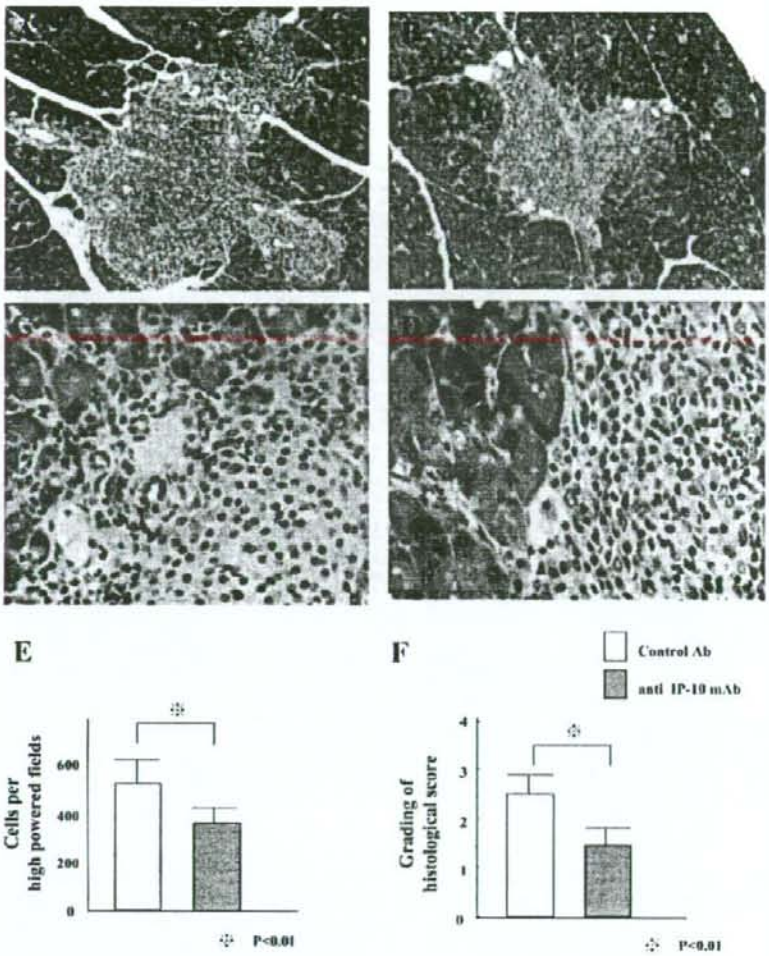

Fig. 5. Amelioration of pancreatic lesions of mice with MAIDS by neutralization of IP-10/CXCL10. *A* and *C*: pancreas from mice infected with LP-BM5 MuLV treated with control Ab at 8 wk after infection; *B* and *D*: pancreas from mice infected with LP-BM5 MuLV treated with anti-IP-10 mAb at 8 wk after infection. Sections were stained with hematoxylin and eosin. Original magnification: ×200 in *A* and *B* and ×400 in *C* and *D*. *E*: numbers of cells infiltrating the pancreas after infection. *F*: histological scores of acinar cell destruction of the pancreas at 8 wk after infection. Cells were counted under a microscope at high-power magnification for 3 different areas/mouse, and data of each time point were collected from 3 mice and compared with each other. *Data are significantly different between mice injected with anti-IP-10 mAb and those injected with control Ab as determined by Student's *t*-test ($P < 0.01$).

shown that β-cells of the islets of Langerhans produce chemokines including IP-10 with preferential attraction to T cells via CXCR3 (7). In our colitis model and those of others, IP-10 expression was confirmed in the colon epithelial cells, and IP-10 neutralization was shown to ameliorate the colitis with decreased $CXCR3^+$ cells in the colon (27, 29). In addition, Sugai et al. (22) reported that IP-10 is expressed on duct epithelial cells in salivary glands of patients with SjS. Contrary to these reports, we could not detect IP-10 expression on acinar cells or duct epithelial cells but found that IP-10 and CXCR3 were mainly expressed on cells in inflammatory foci around pancreatic ducts. Thus the lack of expression of IP-10 on target acinar cells and duct epithelial cells might be attributed to the mild pancreatitis-like injury of mice with MAIDS. Interestingly, IP-10 was also detected on cells localized between the basal laminas that envelope each acinus of a minimal functional unit of the exocrine system of the pancreas (Fig. 3*H*, *A*, *inset*). These cells disappeared together with the decreased numbers of pancreas-infiltrating cells after the neutralization of IP-10 (Fig. 3*H*, *A* and *C*). Therefore, we need to identify the nature of the $IP\text{-}10^+$ cells localized between basal laminas around each acinus, which are supposed to play a pivotal role in the recruitment of $CXCR3^+$ inflammatory cells into the pancreas of mice with MAIDS.

Recently, a Th1 and Th2 imbalance has been considered as one of the important mechanisms in the development of some autoimmune diseases (25). In our previous studies on the experimental models of encephalomyelitis (20), hepatitis (36), and Thy1.1 glomerulonephritis (8), we reported that anti-IP-10 monoclonal antibody treatment did not affect the cytokine environment of Th1/Th2 polarization. Considering these previous reports together with the observations of this study, it is conceivable that the IP-10 neutralization-induced amelioration of the pancreatic lesions of MAIDS did not result from the rectification of the cytokine environment of Th1/Th2 imbalance but rather from blockade of trafficking of inflammatory cells into the pancreas.

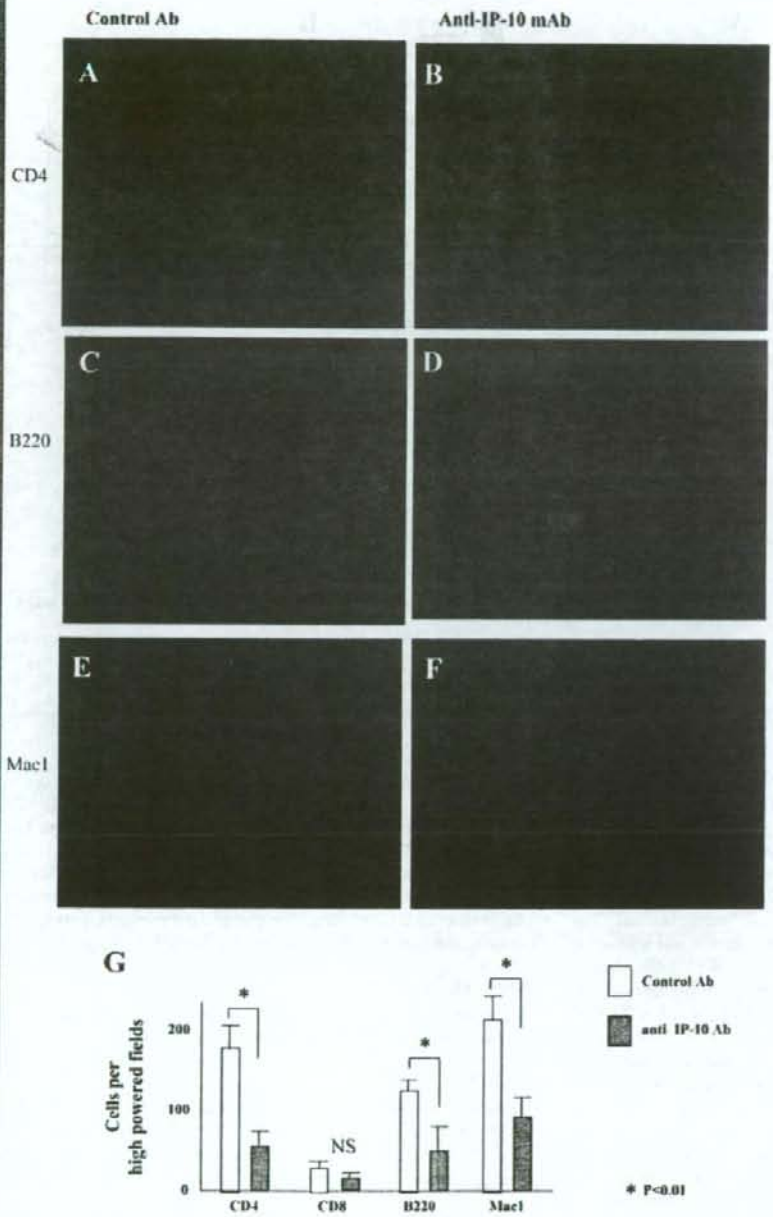

Fig. 6. Effect of neutralization of IP-10/CXCL10 on lymphocyte subpopulations in the pancreas of mice with MAIDS. IF analysis revealed the decreased numbers of CD4 (*A* and *B*), CD8 (data not shown), B220 (*C* and *D*), and Mac-1 (*E* and *F*) immune cells in the pancreas after blockade of IP-10. *G*: quantitative analysis of CD4, CD8, Mac-1, and B220 expression in the pancreas of mice with MAIDS at 8 wk after infection. Each focus of cellular infiltration was examined for the presence of CD4, CD8, B220, and Mac-1 cells. Final results are presented as the numbers of cells per high-powered microscope field. Representative findings (means ± SD; $n = 10$) from 3 independent experiments are shown. *Data are significantly different between mice injected with anti-IP-10 mAb and those injected with control Ab as determined by Student's *t*-test ($P < 0.01$).

In MAIDS, pancreas-infiltrating cells are mainly composed of $CD4^+$T cells, $B220^+$B cells, and Mac-1^+ macrophages (Fig. 6). Neutralization of IP-10 clearly and selectively decreased the numbers of these cells in the pancreas but not in the mLN of mice with MAIDS (Figs. 3–8). Flow cytometric analyses revealed the reciprocal quantitative change of cell phenotype between the mLN and pancreas. That is, IP-10 neutralization increased the numbers of $CD3^+$, $CD4^+$, and $\alpha\beta$T cells as well as Mac-1^+ cells in the mLN but decreased the numbers of those cells in the pancreas of mice with MAIDS (unpublished observations). These results suggest that IP-10 plays a pivotal role in the migration of inflammatory cells between the pancreas and mLN. IP-10-CXCR3 interactions, with Th1-dependent immunity, have been observed in several

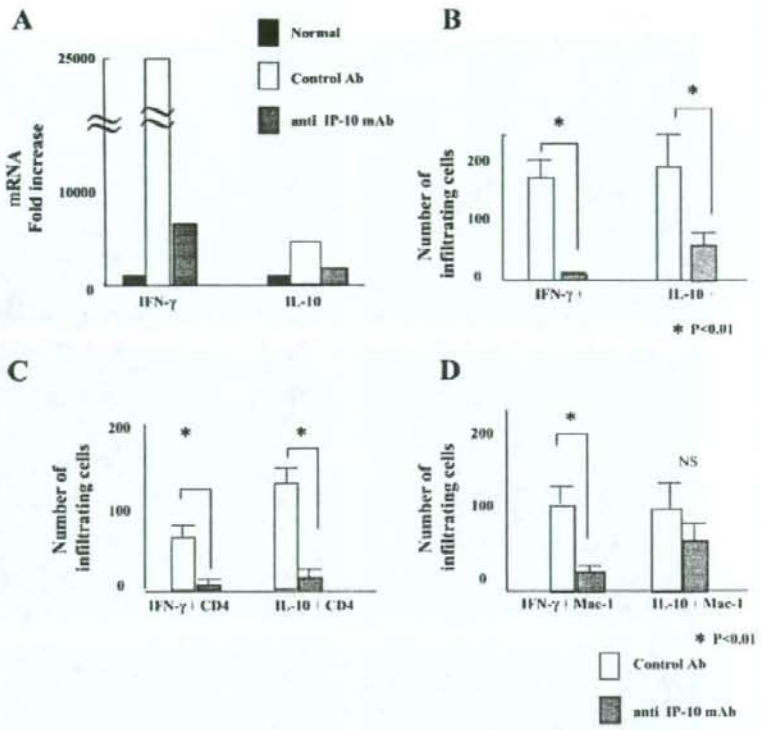

Fig. 7. Effects of blockade of IP-10/CXCL10 on cytokine production by inflammatory cells infiltrating the pancreas in mice with MAIDS. *A*: real-time quantitative PCR of IFN-γ and IL-10 mRNA expression in the pancreas of mice with MAIDS. Each amount was normalized to the level of GAPDH, and the final relative values are expressed relative to calibrators on *day 0*. *B*: numbers of pancreas-infiltrating cells that expressed IFN-γ and IL-10 at 8 wk after infection. Stained cryostat sections of 3 focuses of cellular infiltration of the individual pancreas were examined by counting the numbers of cells expressing IFN-γ and cells expressing IL-10. Three mice were analyzed for each time point. In control normal B6 mice, a negligible number of cells expressed IFN-γ or IL-10, so data are not shown. *C* and *D*: quantitative analysis of IFN-γ and IL-10 expression patterns of $CD4^+$ and Mac-1^+ cells that infiltrated the pancreas at 8 wk after infection. Stained cryostat sections of 3 focuses of cellular infiltration of the individual pancreas were examined by counting the numbers of $CD4^+$ cells expressing IFN-γ or IL-10 (*C*) and Mac-1^+ cells expressing IFN-γ or IL-10 (*D*). Three mice were analyzed for each time point. In control normal B6 mice, a negligible number of cells expressed IFN-γ or IL-10, so data are not shown. *Data are significantly different between mice injected with anti-IP-10 mAb and those injected with control Ab as determined by Student's *t*-test ($P < 0.01$).

inflammatory diseases, including multiple sclerosis (23, 30) and inflammatory bowel diseases (34). In animal models of these diseases, IP-10 neutralization or gene disruption of IP-10 clearly showed that amelioration of the diseases was achieved mainly by blocking $CXCR3^+$ cell trafficking into the IP-10-expressing target organs (5, 27, 29, 36). The ligands CXCL9, CXCL10, and CXCL11 bind to the CXCR3 receptor and share the ability to activate biochemical and functional events in target cells. All these ligands recruit $CXCR3^+$ cells; hence, neutralization of any of these ligands may not be sufficient to significantly abrogate the underlying biology of $CXCR3^+$ cells, but the use of CXCR3-deficient mice and IFN-γ neutralization will elucidate the role of these cells and cytokines in our model in future study. In this study, neutralization of IP-10 decreased not only the numbers of IFN-γ^+ $CD4^+$ T cells but also IL-10^+ $CD4^+$ T and IFN-γ^+ Mac-1^+ cells (Figs. 7 and 8). In an autoimmune diabetic mouse model injected with islet-specific Th1 $CD4^+$ T cells, insulitis was induced by the first accumulation of $CD4^+$ T cells followed by infiltration of Mac-1^+ cells (3). The inflammatory cells that infiltrated initially to the pancreas, therefore, might be the organ-specific autoreactive $CXCR3^+$ IFN-γ^+ $CD4^+$ T cells, and they then produce other cytokines and chemokines to attract the other IL-10^+ $CD4^+$ T cells and IFN-γ^+ Mac-1^+ cells into the pancreas of mice with MAIDS. In this study, we analyzed the effect of IP-10 neutralization only at one time point; however, the effects of the treatment on virus-induced inflammatory infiltrate and cytokine expression are most likely time dependent. Thus we need to analyze the kinetics of the responses in future study. IL-10^+ Mac-1^+ cells in the pancreatic lesions of mice with MAIDS were not significantly reduced by neutralization of IP-10 (Fig. 8), and the function of these cells in the formation of the lesions should be elucidated in future study. In conclusion, IP-10 neutralization could be a unique organ-specific therapeutic strategy for chronic pancreatitis, especially autoimmune pancreatitis associated with SjS.

ACKNOWLEDGMENTS

We thank Dr. Xiu-Hua Yang and Norio Honda for technical assistance and Dr. Minoru Nomoto and Dr. Terasu Honma for helpful discussions.

GRANTS

This work was supported by grants from the Ministry of Education and Science and Technology and the Ministry of Health, Welfare, and Labor of the Government of Japan.

REFERENCES

1. **Baggiolini M.** Chemokines and leukocyte traffic. *Nature* 392: 565–568, 1998.
2. **Bhatia M, Brady M, Shokuhi S, Christmas S, Neoptolemos JP, and Slavin J.** Inflammatory mediators in acute pancreatitis. *J Pathol* 190: 117–125, 2000.
3. **Bradley LM, Asensio VC, Schioetz LK, Harbertson J, Krahl T, Patstone G, Woolf N, Campbell IL, and Sarvetnick N.** Islet-specific Th1, but not Th2, cells secrete multiple chemokines and promote rapid induction of autoimmune diabetes. *J Immunol* 162: 2511–2520, 1999.
4. **Cheung SC, Chattopadhyay SK, Hartley JW, Morse 3rd HC, and Pitha PM.** Aberrant expression of cytokine genes in peritoneal macro-

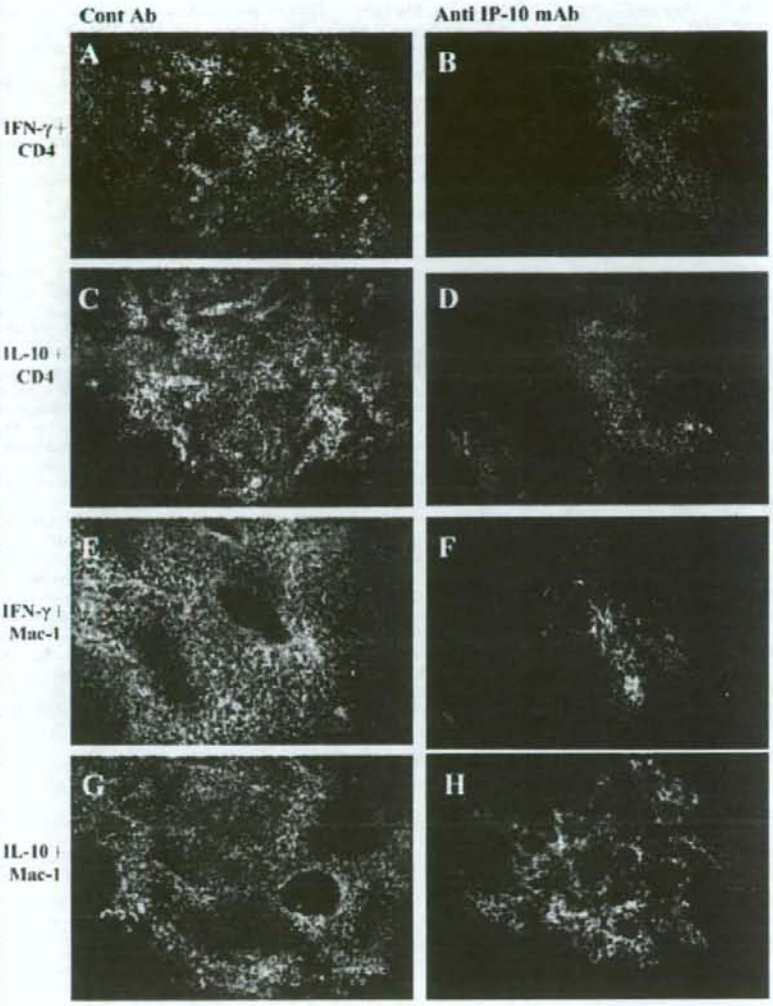

Fig. 8. Effects of blockade of IP-10/CXCL10 by a dual-labeling IF study of cytokine expression with cellular markers in the pancreas of mice with MAIDS. The numbers of cytokine-expressing cells were reduced by neutralization of CXCL10. Shown are sections of the pancreas of mice injected with control Ab (*A*, *C*, *E*, and *G*) or anti-IP-10 mAb (*B*, *D*, *F*, and *H*) at 8 wk after infection. *A–H*: double-color IF staining for CD4 and IFN-γ (*A* and *B*), CD4 and IL-10 (*C* and *D*), Mac-1 and IFN-γ (*E* and *F*), and Mac-1 and IL-10 (*G* and *H*) of the pancreas of mice with MAIDS at 8 wk after infection. *A–D*: CD4 (red); *E–H*: Mac-1 (red); *A*, *B*, *E*, and *F*: IFN-γ (green); *C*, *D*, *G*, and *H*: IL-10 (green).

phages from mice infected with LP-BM5 MuLV, a murine model of AIDS. *J Immunol* 146: 121–127, 1991.

5. **Dufour JH, Dziejman M, Liu MT, Leung JH, Lane TE, and Luster AD.** IFN-γ-inducible protein 10 (IP-10; CXCL10)-deficient mice reveal a role for IP-10 in effector T cell generation and trafficking. *J Immunol* 168: 3195–3204, 2002.
6. **Farber JM.** Mig and IP-10: CXC chemokines that target lymphocytes. *J Leukoc Biol* 61: 246–257, 1997.
7. **Frigerio S, Junt T, Lu B, Gerard C, Zumsteg U, Hollander GA, and Piali L.** β-Cells are responsible for CXCR3-mediated T-cell infiltration in insulitis. *Nat Med* 8: 1414–1420, 2002.
8. **Han GD, Koike H, Nakatsue T, Suzuki K, Yoneyama H, Narumi S, Kobayashi N, Mundel P, Shimizu F, and Kawachi H.** IFN-inducible protein-10 has a differential role in podocyte during Thy1.1 glomerulonephritis. *J Am Soc Nephrol* 14: 3111–3126, 2003.
9. **Hitoshi Y, Okada Y, Sonoda E, Tominaga A, Makino M, Suzuki K, Kinoshita J, Komuro K, Mizuochi T, and Takatsu K.** Delayed progression of a murine retrovirus-induced acquired immunodeficiency syndrome in X-linked immunodeficient mice. *J Exp Med* 177: 621–626, 1993.
10. **Jolicoeur P.** Murine acquired immunodeficiency syndrome (MAIDS): an animal model to study the AIDS pathogenesis. *FASEB J* 5: 2398–2405, 1991.
11. **Kannno H, Nose M, Itoh J, Taniguchi Y, and Kyogoku M.** Spontaneous development of pancreatitis in the MRL/Mp strain of mice in autoimmune mechanism. *Clin Exp Immunol* 89: 68–73, 1992.
12. **Khan IA, MacLean JA, Lee FS, Casciotti L, DeHaan E, Schwartzman JD, and Luster AD.** IP-10 is critical for effector T cell trafficking and host survival in *Toxoplasma gondii* infection. *Immunity* 12: 483–494, 2000.
13. **Kim WK, Tang Y, Kenny JJ, Longo DL, and Morse HC 3rd.** In murine AIDS, B cells are early targets of defective virus and are required for efficient infection and expression of defective virus in T cells and macrophages. *J Virol* 68: 6767–6769, 1994.
14. **Klinken SP, Fredrickson TN, and Hartley JW.** Evolution of B cell lineage lymphomas in mice with a retrovirus-induced immunodeficiency syndrome, MAIDS. *J Immunol* 140: 1123–1131, 1998.
15. **Kubo Y, Nakagawa Y, Kakimi K, Matsui H, Iwashiro M, Kuribayashi K, Masuda T, Hiai H, Hirama T, Yanagawa S, and Ishimoto A.**